Magnetic dichroism in darkfield UV photoemission electron microscopy

Maximilian Paleschke[1], David Huber[1], Friederike Wührl[1], Cheng-Tien Chiang[2], Frank O. Schumann[3], Jürgen Henk[1], Wolf Widdra[1]
[1] *Institute of Physics, Martin Luther University Halle-Wittenberg, D-06099 Halle (Saale), Germany*
[2] *Institute of Atomic and Molecular Sciences, Academia Sinica, Taipei, Taiwan and*
[3] *Max-Planck-Institut für Mikrostrukturphysik, 06120 Halle, Germany**
(Dated: August 5, 2024)

Photoemission electron microscopy (PEEM) has evolved into an indispensable tool for structural and magnetic characterization of surfaces at the nanometer scale. Particularly, synchrotron-radiation-based X-ray PEEM has emerged as a leading method for probing element-specific magnetic properties via magnetic circular dichroism (MCD) in core level photoemission. In laboratory settings, UV radiation is utilized for near-threshold PEEM, which, when combined with femtosecond lasers, offers the potential for ultrafast time resolution. However, the characterization of magnetic properties, such as local magnetic domain structures, has seen limited application in UV-PEEM, with studies reporting only weak magnetic dichroism effects for in-plane magnetization. Here we introduce the concept of darkfield PEEM for MCD in threshold photoemission. This method enables efficient MCD imaging with a significantly enhanced MCD contrast—by an order of magnitude—for in-plane magnetization, as demonstrated for Fe(001). This advancement paves the way for MCD imaging on femtosecond timescales using modern lasers. Darkfield PEEM imaging employs an aperture for photoelectron momentum selection in the back focal plane of the electron imaging column before forming the real-space image. While the general momentum dependence of the MCD contrast will be explained through symmetry considerations, the experimental results for Fe(001) will be quantitatively compared with state-of-the-art full-relativistic photoemission calculations.

Introduction. Ultrafast spin and magnetization dynamics are exciting and rapidly growing fields in condensed matter physics with promising implications for both future research and device applications. Ultrafast imaging of magnetic domains on the micrometer scale is well established based on all-optical methods, as e.g. Kerr microscopy. On the nanometer scale, however, electron microscopy is the method of choice due to electrons short de Broglie wavelength. For imaging magnetic domains the magnetic circular dichroism (MCD) contrast is used in photoelectron emission microscopy (PEEM). The intensity recorded for a particular domain changes with the helicity of the incident radiation, thereby producing magnetic contrast without the need for an explicit electron spin detection. By tuning the incident X-ray radiation to a magnetic core level absorption edge, substantial and element-specific MCD asymmetries have been reported. With the wide availability of tunable synchrotron radiation, this technique of XMCD-PEEM is well established for magnetic domain imaging on the nanometer scale and for slow dynamics [1]. However, the pulse length of synchrotron radiation of typically 30-50 ps renders XMCD-PEEM unsuitable on ultrafast timescales. Replacing the incident X-ray radiation by ultrashort laser pulses solves this issue straightforwardly and allows for pump-probe experiments on a few femtoseconds timescale. In addition, experiments can be performed in the laboratory with UV laser sources, which excite electrons close to the Fermi level to energies slightly above the escape threshold. However, the reported MCD contrasts are quit small in threshold photoemission, especially for in-plane magnetization.

As we demonstrate here, the concept of darkfield PEEM in threshold photoemission allows efficient MCD imaging with an order-of-magnitude enhanced MCD contrast for in-plane magnetization. It paves the way for MCD imaging on femtosecond timescales with modern UV laser sources. Darkfield PEEM imaging uses an aperture for photoelectron momentum selection in the back focal plane of the electron imaging column prior to forming the real space image. We will demonstrate this for the in-plane magnetic structure at the Fe(001) surface and compare quantitatively the experimental results with state-of-the-art full-relativistic photoemission calculations.

Check review of existing literature below

After the first observation and theoretical work of magnetic dichroism in the valence band [2–4], the first experimental evidence of magnetic dichroism in threshold PEEM was reported by Marx *et al.* in 2000 [5]. Their investigation on polycrystalline Fe revealed a linear asymmetry of 0.37 %. After that, many spectroscopic studies followed, showing the existence of circular and linear dichroism in several ferromagnetic materials [6–10]. Nakagawa *et al.* built on the first experimental work of Marx. They chose Ni films adsorbed with Cs, which showed large asymmetries up to 12 % in circular dichroism PEEM for out-of-plane oriented domains [11–13]. This also proved the applicability of pulsed laser light for dichroism imaging. Due to the limited photon energy of commonly available optical laser setups, Cs is still needed in most photoemission experiments to reduce the work function [14, 15]. Notably, domains at the FePt surface were investigated utilizing a pulsed deep-UV laser with a

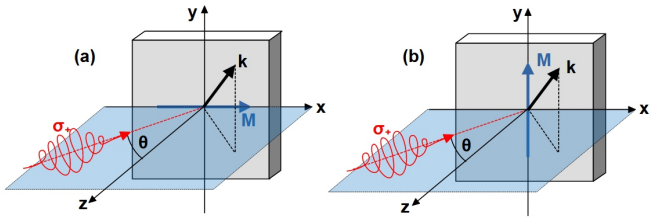

FIG. 1. Symmetry analysis. A circular polarized laser pulse (orange, with helicity σ_+ impinges onto a magnetic domain (rectangular solid). The light incidence direction and the surface normal (z-axis) span the scattering plane (blue; xz-plane) with magnetization direction $\boldsymbol{M}$ oriented within or perpendicular to the scattering plane in (a) and (b), respectively. Note that the off-normal detection of photoelectrons with wavevector $\boldsymbol{k}$ (black arrow) results in a chiral setup.

photon energy of 7 eV [16]. On the other side, the theory of valence-band dichroism was predominately developed in the 90s and early 2000s by Feder, Henk, Kuch, Schneider and Venus [3, 4, 17–20] and supported by pioneering experiments of Tamura, Schmiedekamp, Kirschner, and Hild [7–9, 21–23]. It is based on calculating the relativistic band structure in combination with a theoretical description of the photoemission process.

Do we need to cite Getzlaff'22 [24]?

Conceptual basis. For a simplified conceptual approach we consider a surface with fourfold symmetry, as e.g. the (001) fcc or bcc surfaces with magnetic easy axes along the four [100] directions. Let's assume light incidence along the surface normal (Fig. 1 for $\theta = 0$). The photoemission intensity of electrons detected with off-normal wavevector $\boldsymbol{k}$ depends then on the helicity, σ_+ or σ_-, of the incident circular polarized laser radiation and on the two orientations $\pm M$ of the in-plane magnetization in a selected domain, yielding four intensities $I_{\boldsymbol{k}}(\sigma_\pm, \pm M)$ (shortened $I_{\pm\pm}$). The latter intensities are combined into the total intensity

$$I \equiv I_{++} + I_{+-} + I_{-+} + I_{--}. \tag{1}$$

In order to disentangle the two main contrast mechanisms we define appropriate asymmetries:

$$A_{\mathrm{pol}} \equiv \left[(I_{++} + I_{+-}) - (I_{-+} + I_{--})\right]/I, \tag{2a}$$
$$A_{\mathrm{ex}} \equiv \left[(I_{++} + I_{--}) - (I_{+-} + I_{-+})\right]/I. \tag{2b}$$

In the polarization asymmetry A_{pol} the magnetization's orientation is averaged out; it thus encodes contrast due to the light's helicity, as if the domain were nonmagnetic. Contrast due to the exchange splitting is quantified by the exchange asymmetry A_{ex}, in which one averages over the mutual orientations of helicity and magnetization. Note that the *chiral geometry* for photoelectrons with *off-normal* wavevector $\boldsymbol{k}$ outside the scattering plane results in magnetic dichroism and, hence, in magnetic contrast.

If the scattering plane is a mirror plane of the lattice, the photoemission intensities for fixed $\boldsymbol{k}$ within the scattering plane obey the symmetry relation $I(\sigma_+, +\boldsymbol{M}) = I(\sigma_-, -\boldsymbol{M})$ for a magnetization within the scattering plane (Fig. 1(a)). This results into a finite A_{ex}, but vanishing A_{pol}. For perpendicular magnetization, $I(\sigma_+, +\boldsymbol{M}) = I(\sigma_-, +\boldsymbol{M})$ holds that leads here to vanishing A_{pol} and vanishing A_{ex}.

In the following, we compare the theoretical MCD asymmetries based on relativistic photoemission computations for Fe(001), briefly described in the Supplemental Material [25], with corresponding experimental results for a photon energy of 5.2 eV. The photoemission has been recorded for 70° grazing light incidence within the [100] high-symmetry direction in a standard PEEM setup (Focus GmbH, Hünstetten). As light source either a mercury discharge lamp or the frequency-doubled output of a non-collinear optical amplifier (NOPA) with circular polarization optics is used [26–28].

Contrast mechanisms. The polarization asymmetry A_{pol} as defined in Eq. (2a) and depicted in Fig. 2, depends on the binding energy of the initial states. Both, theoretical (top row) and experimental data (bottom row), show that this contrast mechanism is sizable with absolute values up to about 40 % in theory and 20 % in experiment and thus cannot be ignored. The theoretical patterns (top row in Fig. 2) exhibit two nodal lines at $k_x = 0$ and at $k_y = 0$. Moreover, one finds changes of sign if either k_x or k_y is reversed. These features are imposed by the symmetry of the setup, specifically the off-normal light incidence. The experimental counterparts (bottom row) display the same features but slightly oblique or off-center, most clearly for binding energies with comparably small asymmetry (cf. 0.15 eV and 0.25 eV). We attribute these deviations to imperfections in experiment, for example a small misalignment of the light incidence with respect to a crystal mirror plane. Moreover, we assume an electron self energy that is independent of $k_\parallel$ (see [25]). Nevertheless, the agreement between experiment and theory is remarkable good over the full range of electron binding energies. Note that the experimental asymmetries have been determined from two separate 2D momentum maps for magnetization directions $+\boldsymbol{M}$ and $-\boldsymbol{M}$ with respect to the [100] direction via selection of appropriate single magnetic domains.

The energy-dependent exchange asymmetry A_{ex}, defined in Eq. (2b) and shown in Fig. 3, exhibits absolute values up to 10 % in theory and 6 % in experiment. It exhibits a clear odd symmetry upon reversal of k_x, whereas it does not change sign upon reversal of k_y, in contrast to A_{pol}. Both features are dictated by the symmetry of the setup (see [25]), while the absolute value and the sign of the asymmetries depend on the initial state binding energy via the band structure and photoemission matrix elements.

The above findings support that the asymmetries A_{pol}

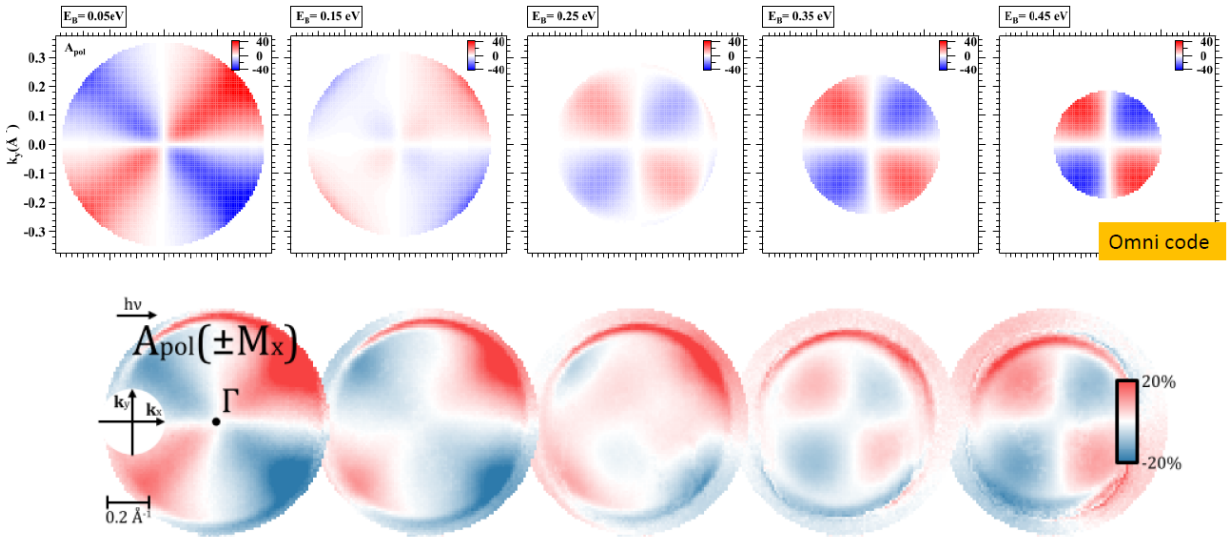

FIG. 2. Polarization asymmetry A_{pol} of Fe(001) at selected binding energies versus wave vector $\boldsymbol{k}_{\parallel}$ of the photoelectrons for 70° grazing light incidence. Top row: theoretical results obtained from photoemission calculations. The binding energy is indicated at each panel. The color scale, showing A_{pol} as defined in Eq. (2a) in percent, is identical for all panels in this row. Bottom row: respective experimental results. The arrow marked $h\nu$ indicates the light incidence direction. Γ is the center of the surface Brillouin zone ($\boldsymbol{k}_{\parallel} = 0$).

and A_{ex} are suitable tools to disentangle and to quantify the main contrast mechanisms for domain imaging.

Domain imaging. From the momentum-resolved A_{ex} pattern in Fig. 3, it follows directly that MCD imaging might reveal strong magnetic contrast in case of *off-normal* electron momentum selection. On the other hand, different momentum contributions will largely cancel without momentum selection or with a momentum selection centered at $k_x = k_y = 0$. The latter has been widely applied and explains small or vanishing magnetic dichroism for in-plane magnetic domains reported so far [5].

To enhance the magnetic contrast, we place a circular contrast aperture in a $\boldsymbol{k}_{\parallel}$ area of high exchange asymmetry: essentially reducing the area of interest in $\boldsymbol{k}_{\parallel}$ space to a "high-exchange" region. This procedure is known as dark-field imaging in optics. Figure 4 (top) shows nine different contrast aperture positions as black circles in $\boldsymbol{k}_{\parallel}$ space, which result in nine corresponding MCD PEEM images of the same Fe(001) surface region (Fig. 4, bottom), which shows in the center a Landau-like pattern of four orthogonal magnetic domains. For the centred aperture marked in red, the MCD contrast almost vanishes. On the other hand, an aperture centered at $k_x > 0$ and $k_y = 0$ results in a drastically increased contrast of 6 % for magnetic domains oriented in +x versus -x direction, whereas the contrast for domains oriented in +y and -y directions (blue arrows) vanishes. Both observations match quantitatively the result of the $\boldsymbol{k}_{\parallel}$ space measurements in Fig. 3(b). Moving the momentum aperture $k_x < 0$ and $k_y = 0$, reverses the contrast of +x and -x domains. As expected, the contrast switches from sensitivity in x direction to y direction when positioning the aperture at $k_x = 0$ and $k_y > 0$ (upper-middle PEEM image in 4). The upper-right measurement shows a diagonal position with $k_x > 0$ and $k_y > 0$, where the different contributions to the MCD signal mix, resulting in four different asymmetry values for the four in-plane magnetization directions.

Check binding energy in caption of Fig. 4

Band structure effects. The size of A_{ex} and, therefore, the MCD contrast in PEEM for near-threshold photoemission depend on the initial state energy as is demonstrated in Fig. 3 and summarized in Fig. 5 (b). A_{ex} reverses sign from about +6 % at the Fermi level to −5.5 % at $E_B = 0.44\,eV$. For larger binding energies, it decreases again with an absolute value below 1 % at 0.65 eV. These momentum- and energy-resolved PEEM data have been crosschecked with higher energy resolution in a second, angle-resolved photoelectron spectroscopy (ARPES) setup described elsewhere [27, 29] and depicted in Fig. 5 (a). They confirm a maximum value of A_{ex} at the Fermi level, as well as a sign change and a negative maximum at $E_B = xx$ eV and xx eV, respectively, with a decreasing for lower binding energies. Note that this observation calls for exact threshold photoexcitation or for an energy-resolved electron detection in order to obtain high MCD signals. Otherwise the positive and negative exchange asymmetries will partly cancel.

While the darkfield scheme of threshold MCD PEEM is broadly applicable, the magnitude of the binding-

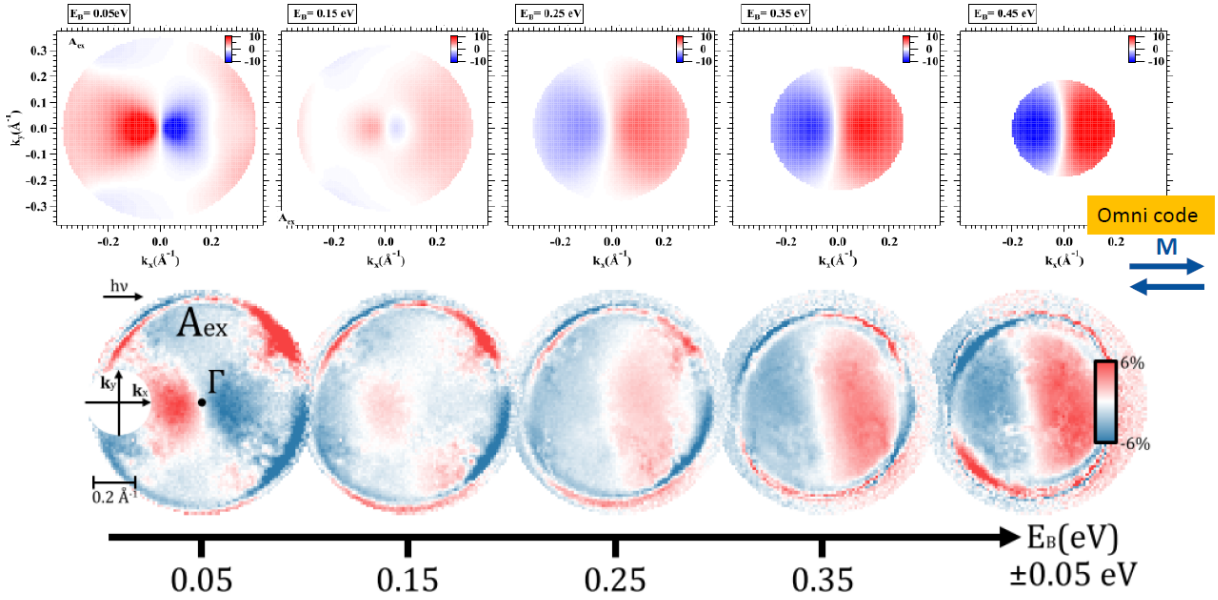

FIG. 3. As Figure 2, but for the exchange asymmetry A_{ex} of Fe(001). The orientations of the magnetization are indicated by arrows on the right-hand side. Note that small differences with respect to an odd symmetry upon reversal of k_x result from grazing light incidence. For normal incidence they are absent.

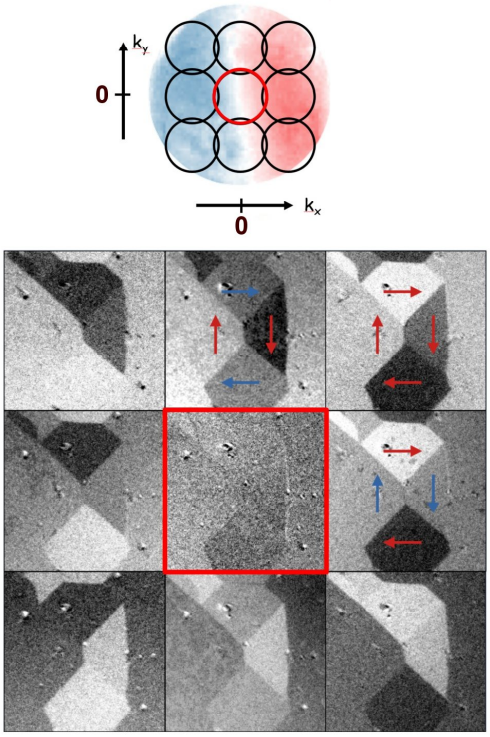

FIG. 4. Darkfield MCD imaging of Fe(100). Top: Schematics of the nine aperture positions in the momentum plane (Momentum-resolved A_{ex} pattern set as background). Bottom: Domain imaging using the nine aperture positions shown above. Photon energy 5.2 eV, grazing light incidence, binding energy xx eV.

FIG. 5. Binding-energy dependent exchange asymmetry A_{ex} for 5.2 eV. (a) ARPES setup with sample magnetized in +x and -x direction (light incidence at 70°, $k_y = 0$). (b) PEEM setup with A_{ex} determined from Fig. 3 (light incidence at 60°, $k_x = xx$ Å, $k_y = 0$).

energy dependent exchange asymmetry A_{ex} is a material-specific property. This property is influenced by the spin-dependent band structure of Fe(001) and the corresponding photoemission matrix elements. It is important to note that these matrix elements are photon energy dependent due to the selection of different photoemission final states.

Summary and prospects. The present investigation proves that magnetic domains can be imaged with high contrast with threshold PEEM using a momentum-selection of the detected photoelectrons as concept of darkfield threshold MCD PEEM.

For a proof-of-principle, we applied darkfield UV PEEM to an in-plane magnetized Fe(001) surface. However, the approach is general so that it can easily be applied to other ferromagnets, even to those with include out-of-plane magnetization [14]. Thus, it is well suited for studying magnetic reorientation transitions, as for example observed for Ni/Cu(001) [6, 14, 30, 31]. We see its main capabilities, however, in investigations of ultrafast magnetization dynamics using femtosecond laser pulses in a optical pump and threshold UV photoemission probe scheme. For applications it paves the way for imaging the ultrafast motion of domain walls [32] or of large skyrmions on nanometer lengthscales [33–35].

Acknowledgments. This work is funded by the Deutsche Forschungsgemeinschaft (DFG, German Research Foundation) – Project-ID 328545488 – TRR 227, projects A06 and B04.

* wolf.widdra@physik.uni-halle.de

[1] W. Kuch, R. Schäfer, P. Fischer, and F. Hillebrecht, *Magnetic Microscopy of Layered Structures*, Springer Series in Surface Sciences, Vol. 57 (Springer, Berlin Heidelberg, 2015).

[2] C. M. Schneider, M. S. Hammond, P. Schuster, A. Ceballada, R. Miranda, and J. Kirschner, Observation of magnetic circular dichroism in uv photoemission from ferromagnetic fcc cobalt films, Physical Review B **44**, 12066 (1991).

[3] J. Henk, T. Scheunemann, S. V. Halilov, and R. Feder, Magnetic dichroism and electron spin polarization in photoemission: Analytical results, Journal of Physics: Condensed Matter **8**, 47 (1996).

[4] R. Feder and J. Henk, Magnetic dichroism and spin polarization in valence band photoemission, in *Spin-Orbit-Influenced Spectroscopies of Magnetic Solids*, Vol. 466, edited by H. Araki, E. Brézin, J. Ehlers, U. Frisch, K. Hepp, R. L. Jaffe, R. Kippenhahn, H. A. Weidenmüller, J. Wess, J. Zittartz, W. Beiglböck, H. Ebert, and G. Schütz (Springer Berlin Heidelberg, Berlin, Heidelberg, 1996) pp. 85–104.

[5] G. K. L. Marx, H. J. Elmers, and G. Schönhense, Magneto-optical Linear Dichroism in Threshold Photoemission Electron Microscopy of Polycrystalline Fe Films, Physical Review Letters **84**, 5888 (2000).

[6] T. Nakagawa and T. Yokoyama, Magnetic Circular Dichroism near the Fermi Level, Physical Review Letters **96**, 237402 (2006).

[7] K. Hild, J. Maul, T. Meng, M. Kallmayer, G. Schönhense, H. J. Elmers, R. Ramos, S. K. Arora, and I. V. Shvets, Optical magnetic circular dichroism in threshold photoemission from a magnetite thin film, J. Phys.: Condens. Matter **20**, 235218 (2008).

[8] K. Hild, J. Maul, G. Schönhense, H. J. Elmers, M. Amft, and P. M. Oppeneer, Magnetic Circular Dichroism in Two-Photon Photoemission, Physical Review Letters **102**, 057207 (2009).

[9] K. Hild, G. Schönhense, H. J. Elmers, T. Nakagawa, T. Yokoyama, K. Tarafder, and P. M. Oppeneer, Energy- and angle-dependent threshold photoemission magnetic circular dichroism from an ultrathin Co/Pt(111) film, Phys. Rev. B **82**, 195430 (2010).

[10] K. Hild, G. Schönhense, H. J. Elmers, T. Nakagawa, T. Yokoyama, K. Tarafder, and P. M. Oppeneer, Dominance of the first excitation step for magnetic circular dichroism in near-threshold two-photon photoemission, Phys. Rev. B **85**, 014426 (2012).

[11] T. Nakagawa, T. Yokoyama, M. Hosaka, and M. Katoh, Measurements of threshold photoemission magnetic dichroism using ultraviolet lasers and a photoelastic modulator, Review of Scientific Instruments **78**, 023907 (2007).

[12] T. Nakagawa, K. Watanabe, Y. Matsumoto, and T. Yokoyama, Magnetic circular dichroism photoemission electron microscopy using laser and threshold photoemission, Journal of Physics: Condensed Matter **21**, 314010 (2009).

[13] T. Nakagawa and T. Yokoyama, Laser induced threshold photoemission magnetic circular dichroism and its application to photoelectron microscope, Journal of Electron Spectroscopy and Related Phenomena **185**, 356 (2012).

[14] M. Kronseder, J. Minár, J. Braun, S. Günther, G. Woltersdorf, H. Ebert, and C. H. Back, Threshold photoemission magnetic circular dichroism of perpendicularly magnetized Ni films on Cu(001): Theory and experiment, Phys. Rev. B **83**, 132404 (2011).

[15] T. N. G. Meier, M. Kronseder, and C. H. Back, Domain-width model for perpendicularly magnetized systems with Dzyaloshinskii-Moriya interaction, Phys. Rev. B **96**, 144408 (2017).

[16] Y. Zhao, H. Lyu, G. Yang, B. Dong, J. Qi, J. Zhang, Z. Zhu, Y. Sun, G. Yu, Y. Jiang, H. Wei, J. Wang, J. Lu, Z. Wang, J. Cai, B. Shen, W. Zhan, F. Yang, S. Zhang, and S. Wang, Direct observation of magnetic contrast obtained by photoemission electron microscopy with deep ultra-violet laser excitation, Ultramicroscopy **202**, 156 (2019).

[17] W. Kuch, A. Dittschar, K. Meinel, M. Zharnikov, C. M. Schneider, J. Kirschner, J. Henk, and R. Feder, Magnetic-circular-dichroism study of the valence states of perpendicularly magnetized Ni(001) films, Phys. Rev. B **53**, 11621 (1996).

[18] W. Kuch and C. M. Schneider, Magnetic dichroism in valence band photoemission, Reports on Progress in Physics **64**, 147 (2001).

[19] D. Venus, Interrelation of magnetic-dichroism effects seen in the angular distribution of photoelectrons from surfaces, Phys. Rev. B **49**, 8821 (1994).

[20] D. Venus, Interpretation of magnetic dichroism in angle-resolved UV photoemission from valence bands, Journal of Magnetism and Magnetic Materials **170**, 29 (1997).

[21] E. Tamura, W. Piepke, and R. Feder, New spin-polarization effect in photoemission from nonmagnetic surfaces, Phys. Rev. Lett. **59**, 934 (1987).

[22] B. Schmiedeskamp, B. Vogt, and U. Heinzmann, Experimental verification of a new spin-polarization effect in photoemission: Polarized photoelectrons from Pt(111) with linearly polarized radiation in normal incidence and normal emission, Phys. Rev. Lett. **60**, 651 (1988).

[23] D. Venus, W. Kuch, A. Dittschar, M. Zharnikov, C. Schneider, and J. Kirschner, Spin-dependent surface transmission in 3d metals: Implications for magnetic-dichroism measurements of the valence bands, Phys. Rev. B **52**, 6174 (1995).

[24] M. Getzlaff, Mcdad investigation to characterize the magnetic behavior of thin pd films on co(0001), Journal of Electron Spectroscopy and Related Phenomena **261**, 147266 (2022).

[25] See Supplemental Material at [URL will be inserted by publisher] for supporting information and additional results.

[26] K. Duncker, M. Kiel, and W. Widdra, Momentum-resolved lifetimes of image-potential states on Ag(001), Surface Science **606**, L87 (2012).

[27] K. Gillmeister, D. Golež, C.-T. Chiang, N. Bittner, Y. Pavlyukh, J. Berakdar, P. Werner, and W. Widdra, Ultrafast coupled charge and spin dynamics in strongly correlated NiO, Nat Commun **11**, 4095 (2020).

[28] M. Paleschke, C.-T. Chiang, L. Brandt, N. Liebing, G. Woltersdorf, and W. Widdra, Plasmonic spin-Hall effect of propagating surface plasmon polaritons in $Ni_{80}Fe_{20}$ microstructures, New J. Phys. **23**, 093006 (2021).

[29] K. Gillmeister, M. Kiel, and W. Widdra, Image potential states at transition metal oxide surfaces: A time-resolved two-photon photoemission study on ultrathin NiO films, Phys. Rev. B **97**, 085424 (2018).

[30] K. Fukumoto, H. Daimon, L. Chelaru, F. Offi, W. Kuch, and J. Kirschner, Micromagnetic properties of the cu/ni crossed-wedge film on cu(001), Surface Science **514**, 151 (2002).

[31] D. Sander, W. Pan, S. Ouazi, J. Kirschner, W. Meyer, M. Krause, S. Muller, L. Hammer, and K. Heinz, Reversible h-induced switching of the magnetic easy axis in ni/cu(001) thin films, Physical Review Letters **93**, 247203 (2004).

[32] S. S. P. Parkin, M. Hayashi, and L. Thomas, Magnetic domain-wall racetrack memory, Science **320**, 190 (2008).

[33] B. Göbel, A. F. Schäffer, J. Berakdar, I. Mertig, and S. S. P. Parkin, Electrical writing, deleting, reading, and moving of magnetic skyrmioniums in a racetrack device, Scientific Reports **9**, 12119 (2019).

[34] H. Jani, J.-C. Lin, J. Chen, J. Harrison, F. Maccherozzi, J. Schad, S. Prakash, C.-B. Eom, A. Ariando, T. Venkatesan, and P. G. Radaelli, Antiferromagnetic half-skyrmions and bimerons at room temperature, Nature **590**, 74 (2021).

[35] L.-M. Kern, B. Pfau, V. Deinhart, M. Schneider, C. Klose, K. Gerlinger, S. Wittrock, D. Engel, I. Will, C. M. Günther, R. Liefferink, J. H. Mentink, S. Wintz, M. Weigand, M.-J. Huang, R. Battistelli, D. Metternich, F. Büttner, K. Höflich, and S. Eisebitt, Deterministic generation and guided motion of magnetic skyrmions by focused he+-ion irradiation, Nano Letters **22**, 4028 (2022).

TODO LIST